ACS Infectious Diseases

pubs.acs.org/journal/aidcbc

Article

Characterization and Noncovalent Inhibition of the Deubiquitinase and deISGylase Activity of SARS-CoV-2 Papain-Like Protease

Brendan T. Freitas, Ian A. Durie, Jackelyn Murray, Jaron E. Longo, Holden C. Miller, David Crich, Robert Jeff Hogan, Ralph A. Tripp, and Scott D. Pegan*

Cite This: https://dx.doi.org/10.1021/acsinfecdis.0c00168

Read Online

ACCESS | Metrics & More | Article Recommendations | Supporting Information

ABSTRACT: Severe acute respiratory syndrome coronavirus 2 (SARS-CoV-2), the causative agent for COVID-19, is a novel human betacoronavirus that is rapidly spreading worldwide. The outbreak currently includes over 3.7 million cases and 260,000 fatalities. As a betacoronavirus, SARS-CoV-2 encodes for a papain-like protease (PLpro) that is likely responsible for cleavage of the coronavirus (CoV) viral polypeptide. The PLpro is also responsible for suppression of host innate immune responses by virtue of its ability to reverse host ubiquitination and ISGylation events. Here, the biochemical activity of SARS-CoV-2 PLpro against ubiquitin (Ub) and interferon-stimulated gene product 15 (ISG15) substrates is evaluated, revealing that the protease has a marked reduction in its ability to process K48 linked Ub substrates compared to its counterpart in SARS-CoV. Additionally, its substrate activity more closely mirrors that of the PLpro from the Middle East respiratory syndrome coronavirus and prefers ISG15s from certain species including humans. Additionally, naphthalene based PLpro inhibitors are shown to be effective at halting SARS-CoV-2 PLpro activity as well as SARS-CoV-2 replication.

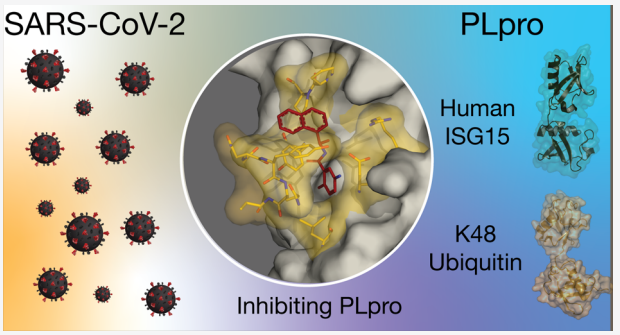

KEYWORDS: *severe acute respiratory syndrome 2, coronavirus, COVID-19, PLpro, ubiquitin, ISG5*

COVID-19 disease is caused by severe acute respiratory syndrome coronavirus 2 (SARS-CoV-2), which was identified in Wuhan, China.[1,2] SARS-CoV-2 is classified as a betacoronavirus from the same species as the severe acute respiratory syndrome coronavirus (SARS-CoV), which was responsible for a pandemic in 2002−2003.[1,3] SARS-CoV-2 has rapidly spread worldwide to over 184 countries with at least 3.6 million cases and >260,000, fatalities according to the latest World Health Organization situation report as of May 6, 2020. The rapid spread of SARS-CoV-2 and its ability to cause death disproportionately in older individuals or individuals with underlying conditions have created an urgent need for antiviral therapeutics and vaccines for use against the virus.[4]

Upon entry into the cell, SARS-CoV-2 and other betacoronaviruses initially translate two polypeptides pp1a and pp1ab that encode up to 16 nonstructural proteins (Nsp1 to Nsp16). Included within this polypeptide are proteins necessary to form the viruses' replicase complex. Once formed, this complex then transcribes the viruses' RNA genome before translation of the viruses' nucleocapsid protein and structural proteins S, E, and M. Lastly, these components are formed into mature virons within the endoplasmic reticulum−Golgi intermediate compartment.[5] One of the essential steps for successful viral replication is the formation of the viral replicase complex through the cleavage of the pp1a and pp1ab polypeptides by two viral proteases.[6,7] One of the main proteases from coronaviruses (CoVs), the 3C-like protease, is known for its ability to cleave Nsp4−Nsp16. In addition to the 3C-like protease, CoVs can also encode for up to two papain-like proteases (PLPs) of which one cleaves Nsp1−3. For example, CoVs such as the mouse hepatitis virus (MHV) and other human coronaviruses including NL63, OC43, HKU1, and 229E encode for a PLP1 and PLP2.[8] The genome of SARS-CoV-2 mirrors that of the Middle East respiratory syndrome CoV (MERS-CoV) and SARS-CoV by coding for a single papain-like protease (PLpro).[8]

Beyond the role of PLpros to cleave the viral polypeptide, PLpros and their PLP2 counterparts in some CoVs have also been observed to suppress host innate immune responses through the reversal of post-translational modification of proteins by ubiquitin (Ub) and interferon-stimulated gene product 15 (ISG15).[7,9] Up to eight different linkage forms of ubiquitination as well as ISGylation events have been observed

Received: March 30, 2020
Published: May 19, 2020

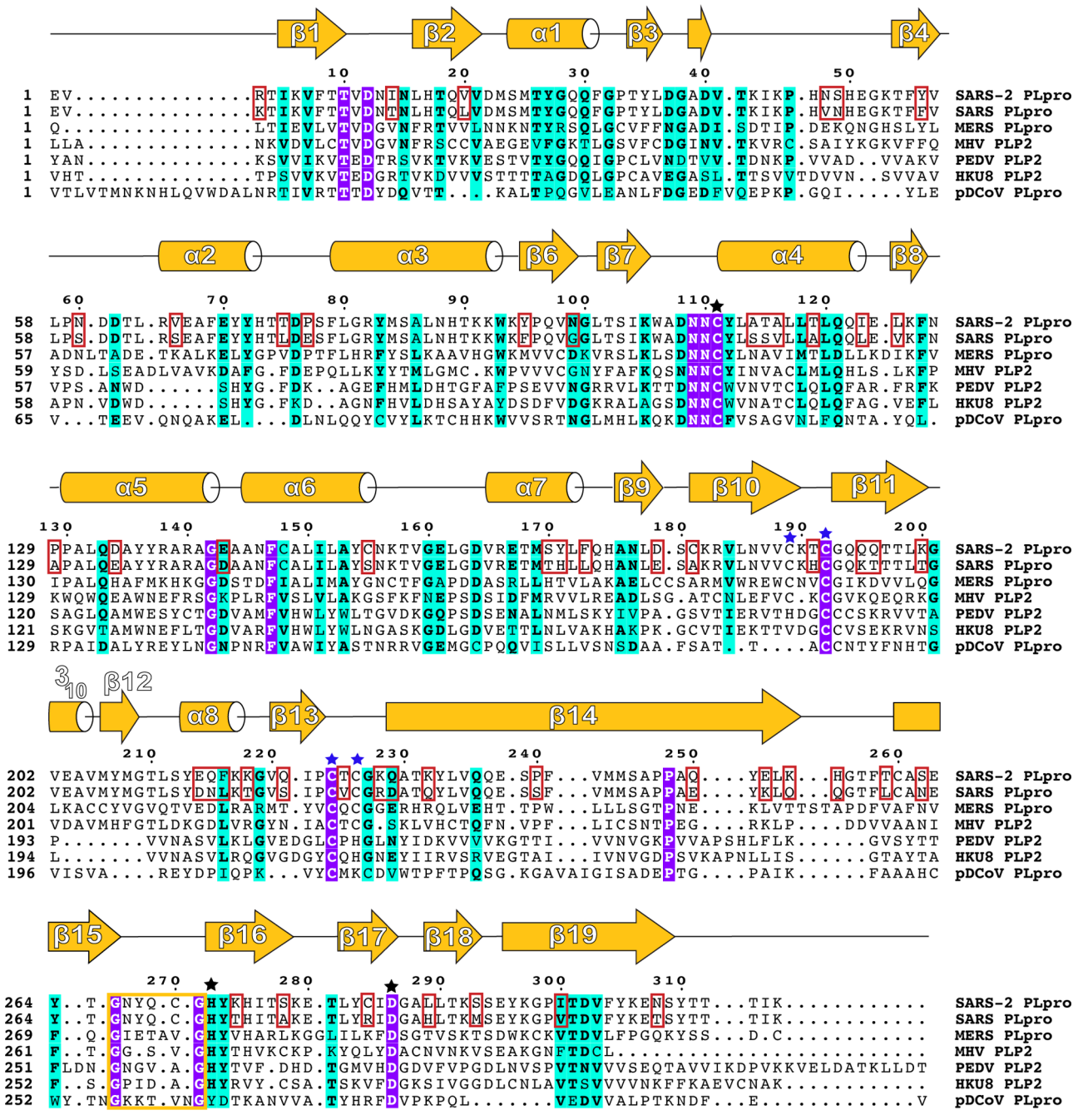

Figure 1. Sequence alignment of PLPs from coronaviruses. The PLpro or PLP from SARS-CoV-2 (accession number MN908947.3), SARS-CoV-1 (accession number P0C6U8), MERS-CoV (accession number AFS88944), HCoV-OC43 (accession number AMK59674), HCoV-229E (accession number APT69896), and HCoV-HKU1 (accession number ARB07606). The secondary structure shown is the predicted by DSSP for SARS-CoV PLpro (5E6J). Similarity and alignment calculations were performed using ClustalW. Residue positions that are fully conserved are marked in purple, with those being highly conserved marked in cyan. Residues that form the catalytic triad are marked with black stars, while residues forming the zinc finger motif are marked with blue stars. The BL2 loop is boxed in gold. The sites of amino acid difference between PLpros of SARS-CoV-1 and SARS-CoV-2 are boxed in red.

to regulate facets of the innate immune defense, which a virus must outpace before the infection is cleared by the adaptive immune system.[10−12] Specifically, modification of host proteins by Ub and ISG15 has been shown to facilitate the NFκB inflammation and IFN-I responses.[13] Also, ubiquitination and ISGylation can upregulate the production of cytokines, chemokines, and other IFN-stimulated gene products with antiviral properties during infection.[13,14] Apart from the modification of host proteins by Ub and ISG15, degradation or sequestration of viral proteins via ISGylation has also been found to play a role in host immunity.[15−17] For PLpros and their PLP2 equivalents, their direct overall impact on CoV pathogenesis has been previously shown to be substantial.[7,13,14,18] Although the exact role of the deISGylating activity of these proteases remains unclear,[19,20] a recent study using an altered MHV PLP2 with ablated deubiquitinase functionality was shown to attenuate pathogenesis in mice. At least part of this reduced pathogenesis for the virus encoding

https://dx.doi.org/10.1021/acsinfecdis.0c00168
ACS Infect. Dis. XXXX, XXX, XXX−XXX

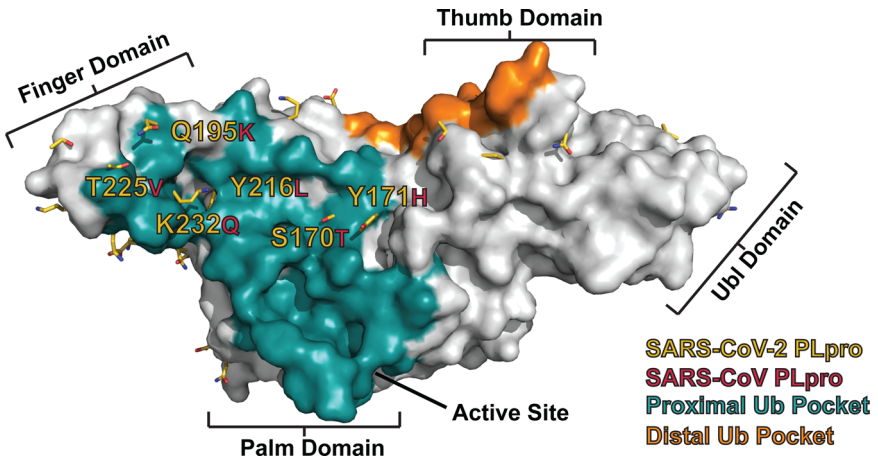

Figure 2. Surface rendering of a SARS-CoV-2 PLpro homology model highlighting its differences with SARS-CoV-1 PLpro. The SARS-CoV-2 PLpro is shown in gray, with the proximal ubiquitin binding site in teal and the distal ubiquitin binding site in orange. Amino acid sites where PLpro differs between SARS-CoV-2 and SARS-CoV are colored in yellow.

for the altered MHV PLP2 was linked to the IFN response being triggered earlier than that under infection by wild-type MHV.[21]

Although the role of these proteases in suppressing the innate immune response is clear, their Ub and ISG15 substrate specificities can vary widely.[7] Differences in substrate specificity for these proteases also extend to the eight different linkage forms of polyubiquitin (poly-Ub).[7,22] PLpros and PLP2s have also been shown to be sensitive to these species−species variations within ISG15 with their preference including ISG15s from species that they productively infect.[8] This has given rise to the suggestion that viral deubiquitinases and deISGylases may differ in effectiveness toward certain innate immune pathways.[7,15,23,24] Recent studies have shown that specificity among PLpros for Ub and ISG15 substrates can be altered with as little as a single amino acid change.[8,19,20] For instance, the ablation in the deubiquitinating activity of MHV PLP2 that leads to a significant change in pathogenesis came through a change of aspartate to alanine at a single location.[21] Overall, the pp1ab from the SARS-CoV-2 Wuhan-Hu-1 isolate (accession number MN908947.3) has an 80% amino acid identity with SARS-CoV-1 (accession number P0C6U8) when determined by NCBI p-blast. Focusing on PLpro, the two viruses share an 83% sequence identity (Figure 1). This raises the prospect that SARS-CoV-2 PLpro may not possess the same deubiquitinating and deISGylating activities as its SARS-CoV counterpart.

The dual viral polypeptide cleavage and immune suppression roles of PLpros have previously made them a sought after target for small molecule antiviral development.[25−27] In 2008, the first classes of noncovalent drug-like inhibitors, now known as naphthalene PLpro inhibitors, were discovered. Certain members of this class of PLpro inhibitors exhibited nanomolar inhibition against SARS-CoV PLpro and could stymie viral replication in the low micromolar range.[3,28] These and other SARS-CoV PLpro based naphthalene inhibitors are promising for their potency and high selectivity for SARS-CoV PLpro over host proteases.[3,26,27] They also demonstrated no cellular toxicity in Vero E6 cells or A549 cells, with some analogs considered to be metabolically stable.[3,26,27] However, they showed no appreciable ability to inhibit PLpros from other circulating CoVs.[3,25−27] With the SARS-CoV outbreak effectively contained in 2003 with no reemergence, the interest in these potential CoV therapeutics had waned. Given the urgent need for SARS-CoV-2 therapies, whether these naphthalene PLpro inhibitors can now serve as a jumping-off point for SARS-CoV-2 antiviral development is an open question.

Here, we show the first biochemical characterization of the deubiquitinating and deISGylating activities of the SARS-CoV-2 PLpro using 7-amino-4-methyl coumarin (AMC) conjugated Ub and ISG15. These studies reveal marked differences in SARS-CoV-2 PLpro's kinetic values for these substrates compared to its SARS-CoV-1 counterpart and explore the protease's ability to cleave the eight different poly-Ub linkages. The preference of SARS-CoV-2 PLpro for certain species' ISG15s is also examined. Lastly, we show that naphthalene PLpro inhibitors designed for SARS-CoV can inhibit SARS-CoV-2 PLpro as well as impede SARS-CoV-2 replication.

RESULTS

Differences between the PLpro from SARS-CoV and SARS-CoV-2 within the UIM. To explore the potential impact of the 54 differences between the PLpros of SARS-CoV and SARS-CoV2 on enzymatic activity, a homology model was constructed of SARS-CoV-2 PLpro encoded by the severe acute respiratory syndrome coronavirus 2 isolate Wuhan-Hu-1 (accession number MN908947.3; Figure 1). The PDB entry 5E6J of SARS-PLpro bound to K-48 di-Ub was chosen as a template to provide the best representation of a SARS-CoV-2 PLpro in a holo open conformation receptive to substrate binding.[18,29] From the surface perspective of the SARS-CoV-2 PLpro homology model, 40 of the 54 difference sites were spread out relatively equally over the fingers, palm, thumb, and UbL domain of the protease (Figures 2a and S1). On closer examination of the SARS-CoV-2 PLpro's ubiquitin interacting motif (UIM) that is known to accommodate both Ub and ISG15, six sites were found to differ in amino acids from those found in its SARS-CoV counterpart. Specifically, the differences on the SARS-CoV-2 surface within the UIM were S170(T), Y171(H), Y216(L), Q195(K), T225(V), and K232(Q) where the equivalent SARS-CoV residues are marked in parentheses. Intriguingly, one of these sites in SARS-CoV-2 PLpro, K232, is equivalant to Q233 in SARS-CoV PLpro. Previously, a mutation Q233E notably diminished the deubiquitinase activity of that PLpro in favor of more

https://dx.doi.org/10.1021/acsinfecdis.0c00168
ACS Infect. Dis. XXXX, XXX, XXX−XXX

robust deISGylase activity.[8] This further suggests that the enzymatic activities of SARS-CoV-2 PLpro may indeed differ from those of the SARS-CoV PLpro.

Deubiquitinase and deISGylase Activity of SARS-CoV-2 PLpro. To ascertain whether the amino acid differences between SARS-CoV-2 PLpro and its SARS-CoV-1 counterpart translate into differences in enzyme kinetics, SARS-CoV-2 PLpro K_M and k_{cat} values for Ub-AMC and ISG15-AMC as well as the last five consensus amino acids between them (RLRGG; peptide-AMC) were determined (Table 1, Figure S2). The enzymatic efficiency of SARS-CoV-2 PLpro for Ub-AMC was 1.3 ± 0.1 μM^{-1} min^{-1} with K_M and k_{cat} values of 7.9 ± 1.4 and 10.1 ± 0.6, respectively. For the ISG15-AMC substrate, the enzymatic efficiency of SARS-CoV-2 PLpro was 10.3 ± 0.5 μM^{-1} min^{-1} with K_M and k_{cat} values of 3.9 ± 0.5 and 40.0 ± 1.8. SARS-CoV-2 PLpro's enzymatic efficiency toward peptide-AMC is 0.0051 μM^{-1} min^{-1} when assessed using first-order kinetics. Compared to published kinetic values of PLpros or its PLP2 equiv from MHV, SARS-CoV, and MERS-CoV, the PLpro of SARS-CoV-2 surprisingly closely mirrors that of PLpro from MERS-CoV. Both have low enzymatic efficiency toward the peptide substrate and are 2500−3500 times more efficient toward the ISG15 substrate. This is in contrast to SARS-CoV-1 PLpro that is only ∼100 times more efficient toward ISG15 substrates. SARS-CoV-2 is ∼10 times more efficient as an deISGylase than as a deubiquitinase. However, SARS-CoV-1 PLpro is still a more robust deISGylase with 3 times better enzymatic efficiency toward ISG15-AMC than SARS-CoV-2. As a deubiqutinase, SARS-CoV-2 appears to have the highest substrate affinity among PLpros with the lowest turnover, which is orthogonal to its SARS-CoV-1 counterpart.

Table 1. Kinetic Analysis of SARS-CoV-2 PLpro with PEP-AMC, Ub-AMC, and ISG15-AMC

	substrate		
	peptide-AMC	Ub-AMC	ISG15-AMC
SARS-CoV-2 PLpro			
k_{cat}/K_m (μM^{-1} min^{-1})		1.3 ± 0.1	10.3 ± 0.5
k_{cat} (min^{-1})	0.0051[a]	10.0 ± 0.8	40.0 ± 1.8
K_m (μM^{-1})		7.9 ± 1.4	3.9 ± 0.5
SARS-CoV-1 PLpro[b]			
k_{cat}/K_m (μM^{-1} min^{-1})		1.5 ± 0.3	28.9 ± 5.3
k_{cat} (min^{-1})	0.3[a]	75.9 ± 8.1	436 ± 40
K_m (μM^{-1})		50.6 ± 7.4	15.1 ± 2.4
MERS-CoV PLpro[b]			
k_{cat}/K_m (μM^{-1} min^{-1})		1.3 ± 0.2	9.9 ± 1.6
k_{cat} (min^{-1})	0.003[a]	18.8 ± 1.2	32.6 ± 1.8
K_m (μM^{-1})		14.3 ± 2.0	3.3 ± 0.5
MHV PLP[c]			
k_{cat}/K_m (μM^{-1} min^{-1})		38.3 ± 6.3	2.3 ± 0.1[a]
k_{cat} (min^{-1})	0.0016[a]	49.8 ± 2.9	
K_m (μM^{-1})		1.3 ± 0.2	

[a]For nonsaturating substrates, k_{app} is calculated to approximate k_{cat}/K_m. [b]The kinetic parameters of SARS-CoV PLpro (pp1ab; 1-315) and MERS-CoV PLpro (pp1ab 1484-1802; 3-322) are from Baez-Santos et al.[38] [c]The kinetic parameters of MHV PLP are from Chen et al.[32]

Poly-Ub Linkage Preferences for SARS-CoV-2 PLpro. In some cases like the viral ovarian domain proteases encoded by nairoviruses, viral deubiquitinases have demonstrated different levels of activity toward the more natural ubiquitin chains than for monomeric Ub-AMC.[30,31] To examine if this is the case for SARS-CoV-2 PLpro, its ability to cleave the eight different linkage types of poly-Ub, K6, K11, K27, K33, K48, K63, and linear was assessed. Similar to previous studies with MHV PLP2, 20 nM of SARS-CoV-2 PLpro was incubated with 10 μM of each di-Ub linkage.[32] No cleavage of any di-Ub moiety by SARS-CoV-2 PLpro was detected after 60 min (Figure S2). Even the use of 10-fold of the enzyme over 120 min failed to result in a detectable di-Ub cleavage event (data not shown). The same was observed for tetrameric K63 linked polyubiquitin. Of the polymeric ubiquitin chains tested, only tetrameric K48 polymeric ubiquitin chains appeared to be cleaved by the protease (Figure 3).

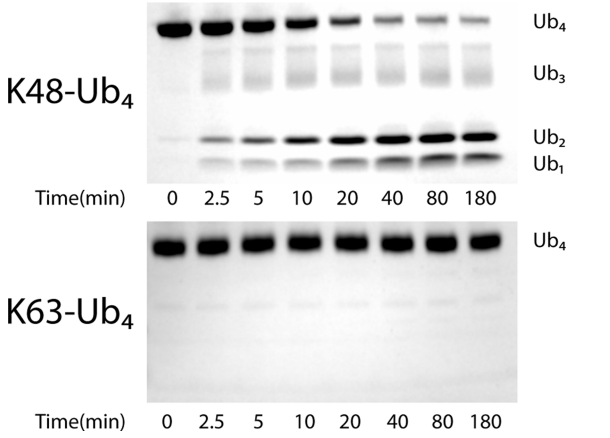

Figure 3. SARS-CoV-2 PLpro preferences for K63 and K48 Ub_4 linkages. Gel cleavage assay of unlabeled K48 amd K63 linked tetra-Ub, visualized by Commassie Blue staining. At 37 °C, 13.7 μM of each Ub moiety was incubated with 23 nM SARS-CoV-2 PLpro for at least 180 min with samples taken at the time points indicated.

SARS-CoV-2 PLpro Exhibits ISG15 Species Preferences. While Ub is almost completely conserved among animals, sequence similarity for ISG15s within the Mammalia class alone can dip below 60%.[33] Only at the genus level do ISG15s from different species appear to have a higher level of similarity[33] (Figure 4a). As this species−species variance in ISG15 has been shown to impact the deISGylase activity of viral deISGylases including PLpros, whether SARS-CoV PLpro followed this phenomenon was explored. Taking advantage of the ability of viral deISGylases to cleave the precursor of ISG15 (proISG15) into mature ISG15,[8,34−36] the ability of SARS-CoV-2 PLpro to cleave the proISG15s from human, vesper bat, pig, mouse, camel, sheep, cow, Egyptian fruit bat, hedgehog, northern tree shrew, and fish was examined. As with other viral deISGylases, SARS-CoV-2 showed a range of ability to successfully engage and process these ISG15 substrates from different species (Figure 4b). Among the 11, the protease appears to prefer ISG15s from sheep and the vesper bat. This is followed by moderate activity for ISG15s from human, pig, camel, and mouse. Weak SARS-CoV-2 PLpro deISGylase activity was observed for the Egyptian fruit bat, hedgehog, and northern tree shrew. No protease activity was observed for the fish pro-ISG15 substrate. Overall, like other viral deISGylases,[8,37] SARS-CoV-2 PLpro appears to be species specific for certain subsets of ISG15s, including at least one ISG15 from species they are known to infect.

https://dx.doi.org/10.1021/acsinfecdis.0c00168
ACS Infect. Dis. XXXX, XXX, XXX−XXX

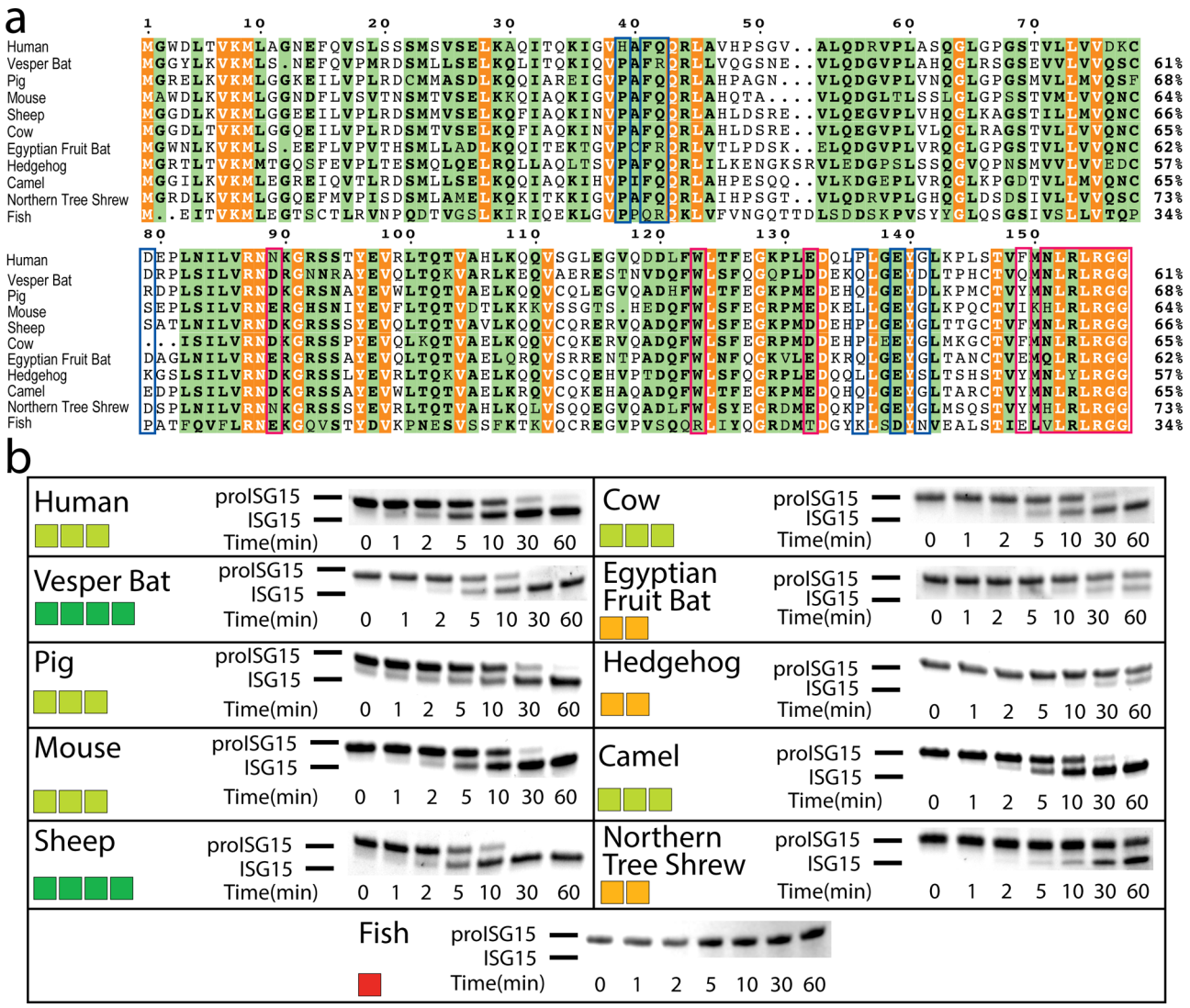

Figure 4. Activity of SARS-CoV-2 PLpro for proISG15 from multiple species. (a) Sequence alignment of ISG15s from human (*Homo sapiens*, accession number AAH09507.1), vesper bat (*Myotis davidii*, accession number ELK23605.1), pig (*Sus scrofa*; accession number ACB87600.1), mouse (*Mus musculus*, accession number AAB02697.1), dromedary camel (*Camelus dromedarius*, accession number XP_010997700.1), sheep (*Ovis aries*, accession number AF152103.1), cow (*Bos taurus*; NP_776791.1), Egyptian fruit bat (*Rousettus aegyptiacus*; XP_015999857.1), hedgehog (*Erinaceus europaeus*; XP_007525810.2), northern tree shrew (*Tupaia belangeri*, accession number AFH66859.1), and jackknife fish (*Oplegnathus fasciatus*, accession number BAJ16365.1). The sequence ruler is based on human ISG15. Similarity and alignment calculations were performed using ClustalW. Residue positions that are fully conserved are marked in orange, with those being highly conserved marked in green. Human ISG15 simliarity to other ISG15s is indicated to the right of the alignment. Red boxes indicate ISG15 amino acid sites known to directly interact with PLpro from SARS-CoV-1 and MERS-CoV.[8,19,20] Blue boxes indicate amino acid sites that have been implied to impact the ISG15 interdomain orientation that can play a role in ISG15-SARS-CoV-1 PLpro engagement.[33] (b) SARS-CoV-2 PLpro was evaluated for the cleavage of proISG15s from the species in (a). At 37 °C, 10 μM of each ISG15 was incubated with 20 nM of SARS-CoV-2 PLpro for at least 1 h with samples taken at the time points indicated. The summary of the proISG15 cleavage assays for different CoV PLPs is presented as a heat map. Colors range from dark red (no cleavage) to green (relatively robust cleavage).

Inhibition of SARS-CoV-2 PLpro by SARS-CoV PLpro Inhibitors. Although SARS-CoV-2 PLpro and SARS-CoV PLpro differ by 54 residues, those lining the active site and nearby P3 and P4 sites are identical (Figure 5a). This includes residues in the BL2 loop that were previously shown to be key in binding naphthalene based PLpro inhibitors.[3,27] To examine whether previously developed SARS-CoV PLpro naphthalene based inhibitors might be effective at inhibiting SARS-CoV-2, five compounds that either had been previously shown to be efficacious or were close analogs were chosen for testing (Figure 5b).[3] Emulating Ratia et al., who detailed the potency of these four compounds against SARS-CoV-1, we utilized the peptide-AMC substrate concentration of 50 μM.[3] The most potent of these four proved to be GRL-0617 with an IC_{50} of 2.4 μM, followed by compound **6** with a low micromolar IC_{50} of 5.0 μM toward SARS-CoV-2. These activities were relatively in line with the 600 nM and 2.6 μM IC_{50} values for GRL-0617 and compound **6**, respectively, reported against SARS-CoV PLpro.[3] The original high-throughput screen lead compounds, 7724772[3] and 6577871,[26] that had 20 μM and 59 μM IC_{50} values against SARS-CoV PLpro presented a similar trend of results with SARS-CoV-2 PLpro. A fifth compound (9247873) was also tested, but no inhibitory effect was observed at 200 μM.

https://dx.doi.org/10.1021/acsinfecdis.0c00168
ACS Infect. Dis. XXXX, XXX, XXX−XXX

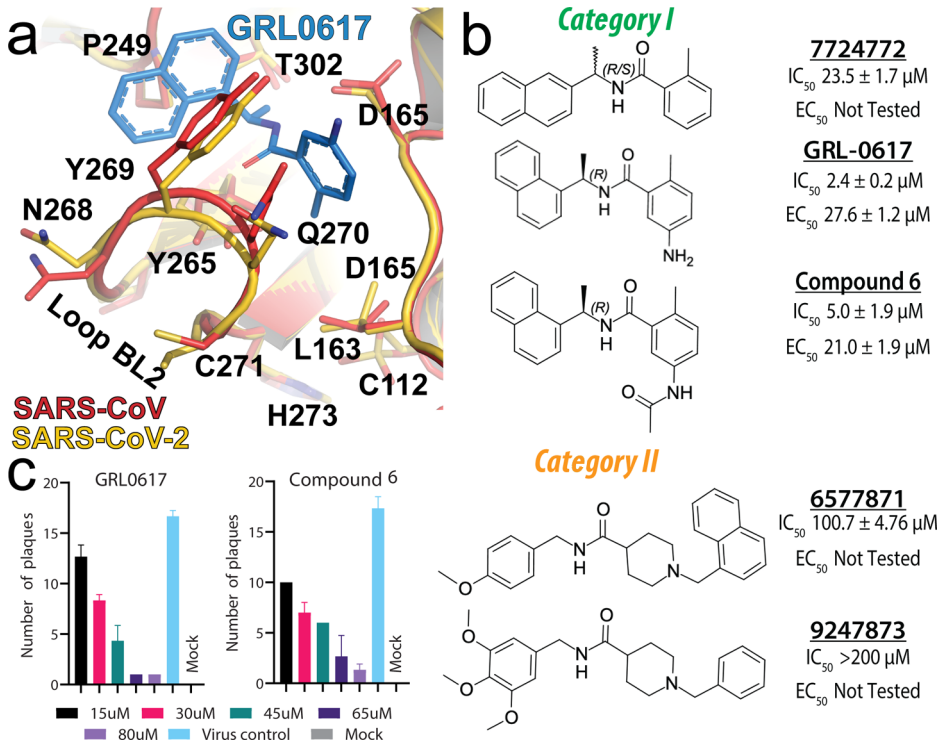

Figure 5. SARS-CoV-2 PLpro model with GRL-0617 as well as enzymatic and antiviral data for PLpro inhibitors against SARS-CoV-2 PLpro and SARS-CoV-2. (a) Comparison of the P3 and P4 substrate binding site of the SARS-CoV-2 PLpro homology model and SARS-CoV counterpart (PDB 3E9S). (b) IC_{50} and EC_{50} values related to the inhibition of SARS-CoV-2 PLpro and SARS-CoV-2 replication by SARS-CoV PLpro inhibitors. (c) SARS-CoV-2 plaque reduction assay data for GRL-0617 and compound **6**. SARS-CoV-2 was incubated with the compounds and assessed 66 h postinfection to determine if the compounds neutralized the virus infection. Plaques were quantified by visual inspection and compared to a nontreated virus control.

Antiviral Activity of SARS-CoV-2 PLpro Inhibition. To examine whether the noncovalent naphthalene based SARS-CoV-2 PLpro inhibitors also possessed antiviral activity for SARS-CoV-2, GRL-0617 and compound **6** were selected for examination against the virus. Plaque reduction assays were performed using Vero E6 cells and the SARS-CoV-2 USA-WA1/2020 isolate to determine the efficacy of inhibiting SARS-CoV-2 PLpro. The SARS-CoV-2 USA-WA1/2020 isolate was readily available, and like other SARS-CoV-2 isolates, its PLpro was fully conserved with the Wuhan-Hu-1 isolate. Excitingly, GRL-0617 and compound **6** exhibited EC_{50} values of 27.6 and 21.0 μM, respectively (Figure 5c). In line with previous studies,[3,27] no cytotoxicity was observed when treating GRL-0617 and compound **6** at the concentrations utilized in this study.

DISCUSSION

Deubiquitinating Activities of SARS-CoV-2 PLpro. The recent revelation that MHV PLP2 deubiquitinase activity is tied to the pathogenesis of this coronavirus by its downregulation of the IFN response mirrors in many ways what was previously observed in the Crimean Congo hemorrhagic fever virus (CCHFV).[15,21] When the CCHFV encoded protease that possessed both deubiquitinase and deISGylase functionality had its deubiquitinase functionality ablated, a more robust IFN response was observed than that with the wild-type virus.[15]

The comparison of SARS-CoV-2 PLpro kinetic parameters to these other two proteases taken from other studies[32,38] highlights that SARS-CoV-2 PLpro appears to perform enzymatically more like MERS-CoV PLpro than its SARS-CoV counterpart (Table 1). Like MERS-CoV PLpro, SARS-CoV-2 PLpro can be readily saturated with Ub-AMC but turns the substrate over substantially more slowly. Although the catalytic efficiency of SARS-CoV-2 PLpro and MERS-CoV PLpro is similar to that of SARS-PLpro for Ub-AMC, their kinetic parameters reveal that they are more susceptible to product inhibition by Ub than their SARS-CoV PLpro equivalent. Given that cellular pools of free ubiquitin in mammalian cells have been found to range from 10 to 23 μM,[39] the overall performance of MERS-CoV and SARS-CoV-2 toward monomeric ubiquitinated substrates in a cellular context could be more divergent than that of SARS-CoV PLpro. In other words, while the PLpro of MERS-CoV and SARS-CoV-2 is at, or near saturating conditions, the PLpro from SARS-CoV-1 is not even at its K_M concentration. The more complex environment of polyubiqutin chain cleavage seems to attest to this difference between the PLpros from MERS-CoV and SARS-CoV-2 versus that of SARS-CoV PLpro. Like MERS-CoV PLpro, SARS-CoV-2 PLpro cleaves K48-linked tetra-Ub at a substantially slower rate than that of SARS-CoV PLpro in previous studies.[38] However, SARS-CoV-2 PLpro is not entirely similar to MERS-CoV in its deubiquitinase activity. Unlike the MERS-CoV protease, SARS-CoV-2 PLpro is similar to its SARS-CoV counterpart in that it shows no appreciable activity for K63 linked polyubiquitin chains.[38]

Given the 83% identity of the SARS-CoV and SARS-CoV-2 at the amino acid level, the appearance of such different deubiquitinating enzymatic profiles between the PLpros

https://dx.doi.org/10.1021/acsinfecdis.0c00168
ACS Infect. Dis. XXXX, XXX, XXX−XXX

encoded by these viruses further highlights that even proteins from viruses within the same species can perform in notably divergent ways. It also highlights some potentially interesting insights from an evolutionary point of view. Among the seven amino acid differences within the UIM, the natural appearance of lysine at SARS-CoV-2 PLpro amino acid site 232 was particularly surprising. The mutation of this equivalent site in SARS-CoV PLpro to glutamate creates an electrostatic repulsion with ubiquitin that diminished that protease's deubiquitinase activities. In SARS-CoV-2, nature appears to have selected for lysine at this position, which should have logically, and appears to have, increased the protease's affinity for Ub at the expense of the overall deubiquitinating functionality. Coronavirus PLpro's activities toward K48-linked ubiquitin have been suggested to counter NF-κB translocation to the nucleus with activity toward K63-linked ubiquitin stymieing others.[27] With viral deubiquitinase activity being a factor in pathogenesis, nature selecting for a viral deubiquitinase with weaker K48 cleavage capability, relatively little K63 cleavage activity, and slower activity toward mono-Ub than its SARS-CoV-1 counterpart at concentrations resembling cellular concentrations may seem counterintuitive at first. However, increased lethality of the host is not necessarily the primary driver of viral evolution, as this can lead to the virus eradicating itself. If nature values successful viral propagation more as a driver, having a weaker viral deubiquitinase may be a better fit. Whether or not this is the case with SARS-CoV-2, which has been able to evade quarantine efforts because of the more often than not initial mild disease symptoms it causes, is an open question. A question whose answer might include virulence factors like PLpros.

SARS-CoV-2 PLpro deISGylasting Activities. As has been found with other PLpros and PLP2s from prominent coronaviruses, SARS-CoV-2 PLpro has a pronounced preference for ISG15 over Ub.[8] Despite the recent insight into the role of these coronavirus protease deubiquitinations, the exact role of viral deISGylase in coronaviruses is a mystery. However, the relatively consistent dominant presence of this type of protease activity among PLpros and PLP2s as well as its demonstrated viral evasion role in other viruses[15] highlights how important coronavirus deISGylase activity maybe for the virus.

Species−species variations in ISG15 have been shown to impact viral replication of influenza B, highlighting the role ISG15 can have on the zoonotic range of influenza B.[40,41] Although it is not known in detail how PLpro deISGylation activity plays a role in coronavirus infection, this activity has been observed to be sensitive to species−species variances within ISG15.[8,33] For instance, PLP2 from MHV can readily process mouse ISG15 substrates but not human ISG15 ones.[8] In the case of MER-CoV PLpro, camel ISG15 is among those species toward which ISG15 has the most activity. The PLpro from SARS-CoV-2 also exhibits this species-specificity phenomenon for its deISGylase activity (Figure 4). It also keeps with the trend set by other viral deISGylases in that it can engage ISG15s from at least the species the virus is known to productively infect: humans.[20,37]

The vesper bat ISG15 was one of the fastest cleaved substrates by SARS-CoV-2; this bat circulates within the Hubei province, lending credence to SARS-CoV-2 originating from bats. However, Egyptian fruit bat ISG15 was cleaved very slowly and did not appear to be a suitable substrate. This is not necessarily surprising as bat ISG15s can have as low as 60% sequence identity and coronaviruses have been seen to be specific to certain bat species.[33,42,43] Whether the vesper bat's presence in the general region from which SARS-CoV-2 originates or if by happenstance vesper bat ISG15 has a similarity at amino acid positions to those of host species for SARS-CoV-2 has a role in the preference requires further investigation.[8,20,37,44]

When compared with SARS-CoV PLpro, the SARS-CoV-2 protease had similar species preferences, particularly in regards to humans, vespers bats, and mice. However, it had slightly higher activity toward sheep and less toward camel.[8] SARS-CoV PLpro also had no activity for fish ISG15 in contrast to its counterparts in MER-CoV, MHV, and SARS-CoV. Although without experimentation all 54 amino acid sites where the two viruses differ could be responsible for this divergence in species-specific deISGylase activity, the 7 divergent sites located within the two viruses' known PLpro-ISG15 interfaces likely hold the most promise. Recently, selective removal of general deISGylase activities from the PLpros of MERS-CoV and SARS-CoV has illuminated the path to molecular tools that can reveal the role that PLpro deISGylase activity has on coronavirus pathogenesis.[8,19,20] This new information that species specificity of SARS-CoV-2 PLpro is not fully conserved with that of its SARS-CoV-1 counterpart may provide a new tool for unraveling the role of viral deISGylastion in coronavirus replication among different hosts, specifically, a SARS-CoV-2 encoding for a PLpro that has been modified to selectively ablate the deISGylase activities of one species in favor of another.

Use of CoV PLpro Inhibitors as a Starting Point for SARS-CoV-2 Therapeutics. Protease inhibitors have a long history of being used as a basis for antiviral therapy, the most salient examples being HIV and Hepatitis C.[45] Within coronaviruses themselves, the main protease inhibitors have been shown to reverse the progression of fatal coronavirus infection.[46] With no therapeutics or vaccines available for the treatment of those infected by SARS-CoV-2, there is an overwhelming need to identify lead compounds that are effective against proposed viral drug targets with SARS-CoV-2. The low micromolar efficacy of GRL-0617 and compound **6** toward SARS-CoV-2 PLpro and the virus itself suggests that previously designed SARS-CoV PLpro inhibitors would be a good place to start. These two compounds as well as the two scaffolds of the five compounds tested represent known noncovalent inhibitor classes of compounds. Additionally, these compounds have been shown to have low cellular toxicity in multiple cell lines,[3,27] and some have displayed the potential to be metabolically stable.[27] Future experiments will need to be performed in additional cell lines as will experiments to tease out some of the pharmacological nuances with the compounds. For now, these scaffolds or others similarly targeting PLpro highlight a viable path to antiviral development and potential use.

CONCLUSIONS

The biochemical characterization of the deubiquitinating and deISGylating activities of SARS-CoV-2 revealed that it more closely resembles that of its counterpart in MERS-CoV than in SARS-CoV. This includes a marked reduction in deubiquitinating activities to include that of cleaving K48-linked tetra-Ub. As with other coronaviruses PLpros and PLP2s, the deISGylating activity of SAR-CoV-2 PLpro appeared to be the more dominant of its various proteolytic functions. This

https://dx.doi.org/10.1021/acsinfecdis.0c00168
ACS Infect. Dis. XXXX, XXX, XXX−XXX

activity also appeared to be species specific only cleaving ISG15 substrates from select species including humans. Although the 54 differences between the PLpros from SARS-CoV and SAR-CoV-2 impacted the proteases functionality, they did not appreciably affect the activity of naphthalene based PLpro inhibitors designed for SARS-CoV efficacy against SARS-CoV-2 from a drug discovery perspective. This revelation offers a potential rapid development path to generating PLpro targeted therapeutics for use against SARS-CoV-2.

METHODS

Chemicals and Reagents. 5-Amino-2-methyl-*N*-[(*R*)-1-(1-naphthyl)ethyl]benzamide (GRL-0617) was purchased from Raystar, CN; 5-(acetylamino)-2-methyl-*N*-[(1*R*)-1-(1-napthanlenyl)ethyl]-benzamide (compound **6**) was purchased from MedChem Express. 2-Methyl-*N*-[1-(2-naphthyl)ethyl]-benzamide (7724772) was purchased from Chembridge; *N*-(4-methoxybenzyl)-1-(1-naphthylmethyl)-4-piperidinecarboxamide oxalate (6577871) was purchased from Chembridge. 1-Benzyl-*N*-(3,4,5-trimethoxybenzyl)-4-piperidinecarboxamide (9247873) was purchased from Chembridge; Z-RLRGG-7-amino-4-methyl-courmarin (peptide-AMC) was purchased from Bachem. Ubiquitin−7-amino-4-methylcourmarin (Ub-AMC) was purchased from Boston Biochem; human ISG15−7-amino-4-methylcourmarin (ISG15-AMC) was purchased from Boston Biochem. Lys6, Lys11, Lys29, Lys33, Lys48, Lys63, and linear linked di-Ub were obtained from Boston Biochem; DL-dithiothroitol (DTT) was purchased from GoldBio, and isopropyl-β-D-thiogalactopyranoside (IPTG) was purchased from GoldBio. 4-(2-Hydroxyethyl)-1-piperazineethanesulfonic acid (HEPES) was purchased from Fisher BioReagents. Imidazole was purchased from Acros Organics; tris(hydroxymethyl)aminomethane (Tris) was purchased from Fisher Scientific. Sodium chloride (NaCl) was purchased from Fisher Chemical, and bovine serum albumin (BSA) was purchased from Sigma Life Science.

Homology Modeling of SARS-CoV-2 PLpro. SARS-CoV-2 PLpro homology models were generated using the MODELLER software suite, version 9.19.[47] For all models, the PLpro from SARS-CoV-2 (accession number MN908947.3) was used as the unknown. The homology model of SARS-CoV-2 PLpro in its holo open form used PDB entry 5E6J as a template, while PDB entry 3E9S was used as a template for the SARS-CoV-2 PLpro homology model used in the docking of GRL-0617. The X-ray structure of 6W9C is now available.

Construction, Expression, and Purification of Viral Deubiquitinases. The ubiquitin-like domain (UbL) and the catalytic core of SARS-CoV-2 PLpro (orf1ab 1564-1876; 1-315) were cloned into pET-15b by Genscript and transformed into T7 express *E. coli*. Cells were cultured in 4.5 L of LB broth containing 100 μg/mL ampicillin at 37 °C until the OD_{600} reached 0.6. Once reached, the expression was induced by the addition of 0.5 mM isopropyl β-D-thiogalactopyranoside (IPTG), and the culture was incubated at 18 °C overnight. The culture was centrifuged at 12 000*g* for 10 min, and the pellet was collected and stored in a −80 °C freezer. The cell pellet was dissolved into lysis buffer (500 mM NaCl and 50 mM Tris-HCl [pH = 7.0]) and then sonicated in Fisher Scientific series 150 on ice at 50% power with 5 s pulses for 6 min. The lysate was centrifuged at 26 000*g* for 45 min to remove all insoluble products. The supernatant was then filtered and placed onto Ni-nitrilotriacetic agarose resin (Qiagen). The resin was washed using five column volumes of lysis buffer containing 10 mM imidazole. The protein was eluted using 5 column volumes of lysis buffer containing 300 mM imidazole. Thrombin was added to the elution to remove the 6X His-tag, and the combined solution was dialyzed in size exclusion buffer (100 mM NaCl, 5 mM HEPES, and 2 mM dithiothreitol (DTT) [pH = 7.4]) and run over a Size Exclusion Superdex 200 column (GE Healthcare, Pittsburgh PA). Purity was confirmed by gel electrophoresis. The Oman strain of the Crimean Congo Hemorrhagic Fever viral ovarian tumor domain protease (1-169) used as a di-Ub control was expressed and purified as previously described.[15]

SARS-CoV-2 PLpro Deubiquitinase and deISGylating Assays. All assays were run using Corning Costar half-volume 96-well plates containing AMC buffer (100 mM NaCl, 50 mM HEPES [pH = 7.5], 0.01 mg/mL bovine serum albumin (BSA), and 5 mM DTT) to a final volume of 50 μL and performed in triplicate. The CLAIROstar plate reader (BMG Lab Tech, Inc.) was used to measure the fluorescence of the AMC cleavage, and the data was analyzed using MARS (BMG Lab Tech, Inc.). The AMC fluorescence was observed from the cleavage of Ub-AMC and ISG15-AMC obtained from Boston Biochem, MA. ISG15-AMC concentrations of substrate ranged from 1 to 15 μM, and Ub-AMC ranged from 0.5 to 30 μM. Protease concentrations used for the Ub-AMC and ISG15-AMC assays were 5 and 0.5 nM, respectively. To calculate K_M and V_{max} values, the initial rates were fitted to the Michalis-Menten equation, $v = V_{max}/(1 + (K_M/[S]))$, using the Enzyme Kinetics (v. 1.3) module of SigmaPlot (v. 10.0, SPSS Inc.). V_{max} was translated into k_{cat} using $k_{cat} = V_{max}/[E]$.

SARS-CoV-2 PLpro Poly-Ub Cleavage Assays. Lys6, Lys11, Lys29, Lys33, Lys48, Lys63, and linear linked di-Ub obtained from Boston Biochem were incubated at 10 μM with 20 nM SARS-CoV-2 PLpro. Reactions were performed in AMC buffer at a volume of 75 μL and a temperature of 37 °C. Ten μL samples were taken at the indicated time points and heat-shocked at 98 °C for 5 min. Lys48 and Lys63 linked tetra-Ub obtained from Boston Biochem were incubated at 13.65 μM with 23 nM SARS-CoV-2 PLpro. Reactions were performed in AMC buffer at a volume of 80 μL and a temperature of 37 °C. Ten μL samples were taken at the indicated time points and heat-shocked at 98 °C for 5 min. SDS-PAGE analysis was performed using Mini-PROTEAN TGX and Coomassie blue.

Protease Activity Assay with proISG15 Substrates. At 37 °C, 20 nM SARS-CoV-2 PLpro was run against 10 μM of each ISG15. Reaction mixtures were 100 μL in PLpro buffer (100 mM NaCl, 5 mM HEPES [pH = 7.4]). Ten μL samples were taken at the indicated time points, and the reaction was quenched in 2× Laemmli sample buffer followed by boiling at 98 °C for 5 min. SDS-PAGE analysis was performed using Mini-PROTEAN TGX Stain-Free.

SARS-CoV-2 PLpro Inhibition IC_{50} Value Determination. IC_{50} assays were performed using similar methods to peptide-AMC, Ub-AMC, and ISG15-AMC cleavage experiments and those described previously.[3] SARS-CoV-2 PLpro was run at 100 nM against 50 μM peptide-AMC in 98% AMC buffer/2% DMSO. Reactions were performed in duplicate with inhibitor concentrations ranging from 1.25 to 20 μM or 100 μM, depending on compound tested. IC_{50} calculations were performed using Prism8 from GraphPad. For 7724772, compound **6**, and GRL-0617, a maximum inhibition of 100%

https://dx.doi.org/10.1021/acsinfecdis.0c00168
ACS Infect. Dis. XXXX, XXX, XXX−XXX

was reached. For 6577871, a maximum inhibition of 61% was reached.

SARS-CoV-2 Antiviral Activity Assays. SARS-CoV-2 (2019-nCoV/USA-WA1/2020; accession number MN985325.1) was received from BEI resources and propagated in Vero clone E6, Vero E6, and CRL-1586. Infections were done at a multiplicity of infection (MOI) of 0.1 in serum-free Dulbecco's minimal essential medium (DMEM) for 1 h after which the virus-containing media was decanted and replaced with DMEM supplemented with 10% heat-inactivated fetal bovine serum.[48] The virus was propagated for 72 h before it was harvested, and the titer was determined by the plaque assay on Vero E6 cells.[49] The viral plaques were counted, and the titer was determined as PFU/mL. The Vero cells were plated at 3×10^5 cells/well in 12-well plates and incubated overnight at 37 °C. The following day, GRL-0617 and compound **6** were prepared at the following concentrations/well in a separate plate; 15, 30, 45, 65, and 80 μM. The cells were washed once with PBS 1× and then infected with 8000 PFU/well with GRL-0617 and compound **6** and incubated for 66 h at 37 °C at 5% CO_2. The cells were then fixed and stained with crystal violet to determine plaque numbers. These were all done in triplicate, and the calculations were performed using Prism8 from GraphPad. A cytotoxicity assessment of compound **6** and GRL-0617 was performed using the Lonza Toxilight bioassay. Vero E6 cells were seeded at 10 000 cells per well and incubated overnight at 37 °C. The plates were washed with 1× PBS, and then, the compounds were added at the specific concentrations and incubated for 72 h. The bioassay was completed following the instructions of the assay, and direct luminometer light output (in relative light units, RLUs) was measured.

■ ASSOCIATED CONTENT

Supporting Information

The Supporting Information is available free of charge at https://pubs.acs.org/doi/10.1021/acsinfecdis.0c00168.

Models of the PLpro anterior side, PLpro activities with substrates, PLpro diubiquitin cleavage gels, and plaque assay plates and cytotoxicity data (PDF)

■ AUTHOR INFORMATION

Corresponding Author

Scott D. Pegan − *Department of Pharmaceutical and Biomedical Sciences, College of Pharmacy, University of Georgia, Athens, Georgia 30602, United States;* orcid.org/0000-0002-2958-5319; Phone: (706)-542-3435; Email: spegan@uga.edu, scott.d.pegan.mil@mail.mil

Authors

Brendan T. Freitas − *Department of Pharmaceutical and Biomedical Sciences, College of Pharmacy, University of Georgia, Athens, Georgia 30602, United States*

Ian A. Durie − *Department of Pharmaceutical and Biomedical Sciences, College of Pharmacy, University of Georgia, Athens, Georgia 30602, United States*

Jackelyn Murray − *Department of Infectious Diseases, College of Veterinary Medicine, University of Georgia, Athens, Georgia 30602, United States*

Jaron E. Longo − *Department of Pharmaceutical and Biomedical Sciences, College of Pharmacy, University of Georgia, Athens, Georgia 30602, United States*

Holden C. Miller − *Department of Pharmaceutical and Biomedical Sciences, College of Pharmacy, University of Georgia, Athens, Georgia 30602, United States*

David Crich − *Department of Pharmaceutical and Biomedical Sciences, College of Pharmacy and Department of Chemistry, Franklin College, University of Georgia, Athens, Georgia 30602, United States;* orcid.org/0000-0003-2400-0083

Robert Jeff Hogan − *Department of Infectious Diseases, College of Veterinary Medicine, University of Georgia, Athens, Georgia 30602, United States*

Ralph A. Tripp − *Department of Infectious Diseases, College of Veterinary Medicine, University of Georgia, Athens, Georgia 30602, United States*

Complete contact information is available at: https://pubs.acs.org/10.1021/acsinfecdis.0c00168

Author Contributions

The manuscript was written through the contributions of all authors. All authors have approved the final version of the manuscript.

Notes

The authors declare the following competing financial interest(s): B.T.F., S.D.P., R.A.T., and R.J.H. have submitted a provisional application U.S.S.N. 62/992,895 pertaining to the work enclosed in the manuscript.

■ ACKNOWLEDGMENTS

The research in the article was partially supported by a grant jointly funded by the University of Georgia College of Pharmacy, Office of Research, and the Department of Pharmaceutical and Biomedical Sciences (S.D.P.). Marvin and ChemAxon products were in part used for the creation of the chemical linker structure, Marvin 6.2.1, 2014 and supported by ChemAxon (http://www.chemaxon.com).

■ ABBREVIATIONS

SARS-CoV-2, severe acute respiratory syndrome coronavirus 2; PLpro, papain-like protease; NSP, nonstructural proteins; CoVs, coronaviruses; PLPs, papain-like proteases; MHV, mouse hepatitis virus; MERS-CoV, Middle East respiratory syndrome CoV; Ub, ubiquitin; ISG15, interferon-stimulated gene product 15; poly ub, polyubiquitin; UIM, ubiquitin interacting motif; AMC, 7-amino-4-methyl coumarin; proISG15, precursor ISG15; CCHFV, Crimean Congo hemorrhagic fever virus; GRL-0617, 5-amino-2-methyl-*N*-benzamide; compound **6**, 5-(acetylamino)-2-methyl-*N*-[(1*R*)-1-(1-napthanlenyl)ethyl]-benzamide; 7724772, 2-methyl-*N*-[1-(2-naphthyl)ethyl]benzamide; 6577871, *N*-(4-methoxybenzyl)-1-(1-naphthylmethyl)-4-piperidinecarboxamide oxalate; 9247873, 1-benzyl-*N*-(3,4,5-trimethoxybenzyl)-4-piperidinecarboxamide; DTT, DL-dithiothreitol; IPTG, Isopropyl β-D-thiogalactopyranoside; HEPES, 4-(2-hydroxyethyl)-1-piperazineethanesulfonic acid; Tris, tris(hydroxymethyl)-aminomethane; BSA, bovine serum albumin; DMSO, dimethyl sulfoxide

■ REFERENCES

(1) Gorbalenya, A. E., Baker, S. C., Baric, R. S., de Groot, R. J., Drosten, C., Gulyaeva, A. A., Haagmans, B. L., Lauber, C., Leontovich,

A. M., Neuman, B. W., Penzar, D., Perlman, S., Poon, L. L. M., Samborskiy, D. V., Sidorov, I. A., Sola, I., and Ziebuhr, J. (2020) Coronaviridae Study Group of the International Committee on Taxonomy of, V. The species Severe acute respiratory syndrome-related coronavirus: classifying 2019-nCoV and naming it SARS-CoV-2. *Nature Microbiology 5*, 536−544.

(2) WHO (2020) *Pneumonia of unknown cause - China*, https://www.who.int/csr/don/05-january-2020-pneumonia-of-unkown-cause-china/en/ (accessed 2020-05-06).

(3) Ratia, K., Pegan, S., Takayama, J., Sleeman, K., Coughlin, M., Baliji, S., Chaudhuri, R., Fu, W., Prabhakar, B. S., Johnson, M. E., Baker, S. C., Ghosh, A. K., and Mesecar, A. D. (2008) A noncovalent class of papain-like protease/deubiquitinase inhibitors blocks SARS virus replication. *Proc. Natl. Acad. Sci. U. S. A. 105*, 16119−16124.

(4) CDC (accessed 2020-05-06) *People Who Are at Higher Risk for Severe Illness*, https://www.cdc.gov/coronavirus/2019-ncov/specific-groups/high-risk-complications.html.

(5) Fehr, A. R., and Perlman, S. (2015) Coronaviruses: an overview of their replication and pathogenesis. *Methods Mol. Biol. (N. Y., NY, U. S.) 1282*, 1−23.

(6) Barretto, N., Jukneliene, D., Ratia, K., Chen, Z., Mesecar, A. D., and Baker, S. C. (2005) The papain-like protease of severe acute respiratory syndrome coronavirus has deubiquitinating activity. *J. Virol. 79*, 15189−15198.

(7) Mielech, A. M., Deng, X., Chen, Y., Kindler, E., Wheeler, D. L., Mesecar, A. D., Thiel, V., Perlman, S., and Baker, S. C. (2015) Murine Coronavirus Ubiquitin-Like Domain Is Important for Papain-Like Protease Stability and Viral Pathogenesis. *J. Virol. 89*, 4907−4917.

(8) Daczkowski, C. M., Dzimianski, J. V., Clasman, J. R., Goodwin, O., Mesecar, A. D., and Pegan, S. D. (2017) Structural Insights into the Interaction of Coronavirus Papain-Like Proteases and Interferon-Stimulated Gene Product 15 from Different Species. *J. Mol. Biol. 429*, 1661−1683.

(9) Ratia, K., Saikatendu, K. S., Santarsiero, B. D., Barretto, N., Baker, S. C., Stevens, R. C., and Mesecar, A. D. (2006) Severe acute respiratory syndrome coronavirus papain-like protease: Structure of a viral deubiquitinating enzyme. *Proc. Natl. Acad. Sci. U. S. A. 103*, 5717−5722.

(10) Zhao, C., Denison, C., Huibregtse, J. M., Gygi, S., and Krug, R. M. (2005) Human ISG15 conjugation targets both IFN-induced and constitutively expressed proteins functioning in diverse cellular pathways. *Proc. Natl. Acad. Sci. U. S. A. 102*, 10200−10205.

(11) Davis, M. E., and Gack, M. U. (2015) Ubiquitination in the antiviral immune response. *Virology 479−480*, 52−65.

(12) Sadler, A. J., and Williams, B. R. (2008) Interferon-inducible antiviral effectors. *Nat. Rev. Immunol. 8*, 559−568.

(13) Frieman, M., Ratia, K., Johnston, R. E., Mesecar, A. D., and Baric, R. S. (2009) Severe acute respiratory syndrome coronavirus papain-like protease ubiquitin-like domain and catalytic domain regulate antagonism of IRF3 and NF-kappaB signaling. *J. Virol. 83*, 6689−6705.

(14) Devaraj, S. G., Wang, N., Chen, Z., Chen, Z., Tseng, M., Barretto, N., Lin, R., Peters, C. J., Tseng, C.-T. K., Baker, S. C., and Li, K. (2007) Regulation of IRF-3-dependent Innate Immunity by the Papain-like Protease Domain of the Severe Acute Respiratory Syndrome Coronavirus. *J. Biol. Chem. 282*, 32208−32221.

(15) Scholte, F. E. M., Zivcec, M., Dzimianski, J. V., Deaton, M. K., Spengler, J. R., Welch, S. R., Nichol, S. T., Pegan, S. D., Spiropoulou, C. F., and Bergeron, E. (2017) Crimean-Congo Hemorrhagic Fever Virus Suppresses Innate Immune Responses via a Ubiquitin and ISG15 Specific Protease. *Cell Rep. 20*, 2396−2407.

(16) Zhao, C., Sridharan, H., Chen, R., Baker, D. P., Wang, S., and Krug, R. M. (2016) Influenza B virus non-structural protein 1 counteracts ISG15 antiviral activity by sequestering ISGylated viral proteins. *Nat. Commun. 7*, 12754.

(17) Dzimianski, J. V., Scholte, F. E. M., Bergeron, E., and Pegan, S. D. (2019) ISG15: It's Complicated. *J. Mol. Biol. 431*, 4203−4216.

(18) Bailey-Elkin, B. A., Knaap, R. C., Johnson, G. G., Dalebout, T. J., Ninaber, D. K., van Kasteren, P. B., Bredenbeek, P. J., Snijder, E. J., Kikkert, M., and Mark, B. L. (2014) Crystal structure of the Middle East respiratory syndrome coronavirus (MERS-CoV) papain-like protease bound to ubiquitin facilitates targeted disruption of deubiquitinating activity to demonstrate its role in innate immune suppression. *J. Biol. Chem. 289*, 34667−34682.

(19) Clasman, J. R., Everett, R. K., Srinivasan, K., and Mesecar, A. D. (2020) Decoupling deISGylating and deubiquitinating activities of the MERS virus papain-like protease. *Antiviral Res. 174*, 104661.

(20) Daczkowski, C. M., Goodwin, O. Y., Dzimianski, J. V., Farhat, J. J., and Pegan, S. D. (2017) Structurally Guided Removal of DeISGylase Biochemical Activity from Papain-Like Protease Originating from Middle East Respiratory Syndrome Coronavirus. *J. Virol. 91*, e01067-17.

(21) Deng, X., Chen, Y., Mielech, A. M., Hackbart, M., Kesely, K. R., Mettelman, R. C., O'Brien, A., Chapman, M. E., Mesecar, A. D., and Baker, S. C. (2020) Structure-Guided Mutagenesis Alters Deubiquitinating Activity and Attenuates Pathogenesis of a Murine Coronavirus. *J. Virol.*, e01734-19.

(22) Ratia, K., Kilianski, A., Baez-Santos, Y. M., Baker, S. C., and Mesecar, A. (2014) Structural Basis for the Ubiquitin-Linkage Specificity and deISGylating Activity of SARS-CoV Papain-Like Protease. *PLoS Pathog. 10*, No. e1004113.

(23) Frias-Staheli, N., Giannakopoulos, N. V., Kikkert, M., Taylor, S. L., Bridgen, A., Paragas, J., Richt, J. A., Rowland, R. R., Schmaljohn, C. S., Lenschow, D. J., Snijder, E. J., Garcia-Sastre, A., and Virgin, H. W. t. (2007) Ovarian tumor domain-containing viral proteases evade ubiquitin- and ISG15-dependent innate immune responses. *Cell Host Microbe 2*, 404−416.

(24) van Kasteren, P. B., Bailey-Elkin, B. A., James, T. W., Ninaber, D. K., Beugeling, C., Khajehpour, M., Snijder, E. J., Mark, B. L., and Kikkert, M. (2013) Deubiquitinase function of arterivirus papain-like protease 2 suppresses the innate immune response in infected host cells. *Proc. Natl. Acad. Sci. U. S. A. 110*, E838−847.

(25) Lee, H., Lei, H., Santarsiero, B. D., Gatuz, J. L., Cao, S., Rice, A. J., Patel, K., Szypulinski, M. Z., Ojeda, I., Ghosh, A. K., and Johnson, M. E. (2015) Inhibitor recognition specificity of MERS-CoV papain-like protease may differ from that of SARS-CoV. *ACS Chem. Biol. 10*, 1456−1465.

(26) Báez-Santos, Y. M., Barraza, S. J., Wilson, M. W., Agius, M. P., Mielech, A. M., Davis, N. M., Baker, S. C., Larsen, S. D., and Mesecar, A. D. (2014) X-ray structural and biological evaluation of a series of potent and highly selective inhibitors of human coronavirus papain-like proteases. *J. Med. Chem. 57*, 2393−2412.

(27) Báez-Santos, Y. M., St. John, S. E., and Mesecar, A. D. (2015) The SARS-coronavirus papain-like protease: structure, function and inhibition by designed antiviral compounds. *Antiviral Res. 115*, 21−38.

(28) Ghosh, A. K., Takayama, J., Aubin, Y., Ratia, K., Chaudhuri, R., Baez, Y., Sleeman, K., Coughlin, M., Nichols, D. B., Mulhearn, D. C., Prabhakar, B. S., Baker, S. C., Johnson, M. E., and Mesecar, A. D. (2009) Structure-based design, synthesis, and biological evaluation of a series of novel and reversible inhibitors for the severe acute respiratory syndrome-coronavirus papain-like protease. *J. Med. Chem. 52*, 5228−5240.

(29) Békés, M., van der Heden van Noort, G. J., Ekkebus, R., Ovaa, H., Huang, T. T., and Lima, C. D. (2016) Recognition of Lys48-Linked Di-ubiquitin and Deubiquitinating Activities of the SARS Coronavirus Papain-like Protease. *Mol. Cell 62*, 572−585.

(30) Capodagli, G. C., Deaton, M. K., Baker, E. A., Lumpkin, R. J., and Pegan, S. D. (2013) Diversity of Ubiquitin and ISG15 Specificity among Nairoviruses' Viral Ovarian Tumor Domain Proteases. *Journal of Virology 87*, 3815−3827.

(31) Dzimianski, J. V., Beldon, B. S., Daczkowski, C. M., Goodwin, O. Y., Scholte, F. E. M., Bergeron, E., and Pegan, S. D. (2019) Probing the impact of nairovirus genomic diversity on viral ovarian tumor domain protease (vOTU) structure and deubiquitinase activity. *PLoS Pathog. 15*, No. e1007515.

(32) Chen, Y., Savinov, S. N., Mielech, A. M., Cao, T., Baker, S. C., and Mesecar, A. D. (2015) X-ray Structural and Functional Studies of the Three Tandemly Linked Domains of Non-structural Protein 3

https://dx.doi.org/10.1021/acsinfecdis.0c00168
ACS Infect. Dis. XXXX, XXX, XXX−XXX

(nsp3) from Murine Hepatitis Virus Reveal Conserved Functions. *J. Biol. Chem. 290*, 25293−25306.
(33) Langley, C., Goodwin, O., Dzimianski, J. V., Daczkowski, C. M., and Pegan, S. D. (2019) Structure of interferon-stimulated gene product 15 (ISG15) from the bat species Myotis davidii and the impact of interdomain ISG15 interactions on viral protein engagement. *Acta Crystallogr. D Struct Biol. 75*, 21−31.
(34) Daczkowski, C. M., Goodwin, O. Y., Dzimianski, J. V., Farhat, J. J., and Pegan, S. D. (2017) Structurally Guided Removal of DeISGylase Biochemical Activity from Papain-Like Protease Originating from Middle East Respiratory Syndrome Coronavirus. *J. Virol. 91*, e01067-17.
(35) Deaton, M. K., Dzimianski, J. V., Daczkowski, C. M., Whitney, G. K., Mank, N. J., Parham, M. M., Bergeron, E., and Pegan, S. D. (2016) Biochemical and Structural Insights into the Preference of Nairoviral DeISGylases for Interferon-Stimulated Gene Product 15 Originating from Certain Species. *J. Virol. 90*, 8314−8327.
(36) Deaton, M. K., Spear, A., Faaberg, K. S., and Pegan, S. D. (2014) The vOTU domain of highly-pathogenic porcine reproductive and respiratory syndrome virus displays a differential substrate preference. *Virology 454*−*455*, 247−253.
(37) Dzimianski, J. V., Scholte, F. E. M., Williams, I. L., Langley, C., Freitas, B. T., Spengler, J. R., Bergeron, E., and Pegan, S. D. (2019) Determining the molecular drivers of species-specific interferon-stimulated gene product 15 interactions with nairovirus ovarian tumor domain proteases. *PLoS One 14*, No. e0226415.
(38) Baez-Santos, Y. M., Mielech, A. M., Deng, X., Baker, S., and Mesecar, A. D. (2014) Catalytic function and substrate specificity of the papain-like protease domain of nsp3 from the Middle East respiratory syndrome coronavirus. *J. Virol. 88*, 12511−12527.
(39) Kaiser, S. E., Riley, B. E., Shaler, T. A., Trevino, R. S., Becker, C. H., Schulman, H., and Kopito, R. R. (2011) Protein standard absolute quantification (PSAQ) method for the measurement of cellular ubiquitin pools. *Nat. Methods 8*, 691−696.
(40) Sridharan, H., Zhao, C., and Krug, R. M. (2010) Species specificity of the NS1 protein of influenza B virus: NS1 binds only human and non-human primate ubiquitin-like ISG15 proteins. *J. Biol. Chem. 285*, 7852−7856.
(41) Versteeg, G. A., Hale, B. G., van Boheemen, S., Wolff, T., Lenschow, D. J., and García-Sastre, A. (2010) Species-specific antagonism of host ISGylation by the influenza B virus NS1 protein. *J. Virol. 84*, 5423−5430.
(42) van Doremalen, N., Schafer, A., Menachery, V. D., Letko, M., Bushmaker, T., Fischer, R. J., Figueroa, D. M., Hanley, P. W., Saturday, G., Baric, R. S., and Munster, V. J. (2018) SARS-Like Coronavirus WIV1-CoV Does Not Replicate in Egyptian Fruit Bats (Rousettus aegyptiacus). *Viruses 10*, 727.
(43) Wang, P. F., Li, Y., Qian, Z. H., Li, J. X., and Ge, X. J. (2018) Isolation and characterization of microsatellite loci from Pterocarya stenoptera (Juglandaceae). *Appl. Plant Sci. 6*, No. e01205.
(44) Jiang, T., and Feng, J. (accessed 2020-05-06) *Myotis davidii. The IUCN Red List of Threatened Species 2019: e.T136250A22003049*, https://dx.doi.org/10.2305/IUCN.UK.2019-3.RLTS.T136250A22003049.en.
(45) Agbowuro, A. A., Huston, W. M., Gamble, A. B., and Tyndall, J. D. A. (2018) Proteases and protease inhibitors in infectious diseases. *Med. Res. Rev. 38*, 1295−1331.
(46) Kim, Y., Liu, H., Galasiti Kankanamalage, A. C., Weerasekara, S., Hua, D. H., Groutas, W. C., Chang, K. O., and Pedersen, N. C. (2016) Reversal of the Progression of Fatal Coronavirus Infection in Cats by a Broad-Spectrum Coronavirus Protease Inhibitor. *PLoS Pathog. 12*, No. e1005531.
(47) Webb, B., and Sali, A. (2017) Protein Structure Modeling with MODELLER. *Methods Mol. Biol. 1654*, 39−54.
(48) Harcourt, J., Tamin, A., Lu, X., Kamili, S., Sakthivel, S. K., Murray, J., Queen, K., Tao, Y., Paden, C. R., Zhang, J., Li, Y., Uehara, A., Wang, H., Goldsmith, C., Bullock, H. A., Wang, L., Whitaker, B., Lynch, B., Gautam, R., Schindewolf, C., Lokugamage, K. G., Scharton, D., Plante, J. A., Mirchandani, D., Widen, S. G., Narayanan, K., Makino, S., Ksiazek, T. G., Plante, K. S., Weaver, S. C., Lindstrom, S., Tong, S., Menachery, V. D., and Thornburg, N. J. (2020) Severe Acute Respiratory Syndrome Coronavirus 2 from Patient with 2019 Novel Coronavirus Disease, United States. *Emerging Infect. Dis. 26*, 1266.
(49) Zhang, Y., Wei, Y., Li, J., and Li, J. (2012) Development and optimization of a direct plaque assay for human and avian metapneumoviruses. *J. Virol. Methods 185*, 61−68.

https://dx.doi.org/10.1021/acsinfecdis.0c00168
ACS Infect. Dis. XXXX, XXX, XXX−XXX